

## Aspects of the dark dimension in cosmology

Luis A. Anchordoqui,<sup>1,2,3</sup> Ignatios Antoniadis,<sup>4,5</sup> and Dieter Lüst<sup>6,7</sup>

<sup>1</sup>*Department of Physics and Astronomy, Lehman College, City University of New York,  
New York 10468, USA*

<sup>2</sup>*Graduate Center, City University of New York, New York 10016, USA*

<sup>3</sup>*Department of Astrophysics, American Museum of Natural History, New York 10024, USA*

<sup>4</sup>*Department of Physics, Harvard University, Cambridge, Massachusetts 02138, USA*

<sup>5</sup>*Laboratoire de Physique Théorique et Hautes Énergies—LPTHE, Sorbonne Université,  
CNRS, 4 Place Jussieu, 75005 Paris, France*

<sup>6</sup>*Max-Planck-Institut für Physik, Werner-Heisenberg-Institut, 80805 München, Germany*

<sup>7</sup>*Arnold Sommerfeld Center for Theoretical Physics, Ludwig-Maximilians-Universität München,  
80333 München, Germany*



(Received 23 December 2022; accepted 13 April 2023; published 27 April 2023)

It was recently understood that if the swampland conjectures are confronted to experiment they naturally point to a solution of the cosmological hierarchy problem in which the smallness of the dark energy is ascribed to an internal (dark) dimension with characteristic length scale in the micron range. It was later inferred that the universal coupling of the Standard Model fields to the massive spin-2 Kaluza-Klein (KK) excitations of the graviton in the dark dimension leads to a dark-matter candidate. Since the partial decay widths of KK gravitons into the visible sector must be relatively small to accommodate experiment, the model is particularly challenging to probe. We show that the model can accommodate neutrino masses associated to right-handed neutrinos propagating in the bulk of the dark dimension with an additional constraint imposed by neutrino oscillation data. After that, we study the impact of the KK tower in cosmology. We show that the modulation of redshifted 21-cm lines driven by  $\text{KK} \rightarrow \gamma\gamma$  could be within the reach of next generation experiments (e.g., SKA and FARSIDE). We also show that indirect dark-matter searches could uncover the  $\text{KK} \rightarrow \gamma\gamma$  signal. These two observations combined have the potential for model identification. Finally, we explore the global structure of the inflationary phase and demonstrate that the model parameters required for a successful uniform inflation driven by a five-dimensional cosmological constant (corresponding to a flat region of the five-dimensional potential) are natural.

DOI: [10.1103/PhysRevD.107.083530](https://doi.org/10.1103/PhysRevD.107.083530)

## I. INTRODUCTION

It was recently pointed out that combining the distance conjectures [1,2] of the Swampland program [3] with the smallness of the dark energy in Planck units ( $\Lambda \sim 10^{-120} M_{\text{Pl}}^4$ ) and confronting these ideas to experiment [4–6] lead to the prediction of a compact dark dimension with characteristic length scale in the micron range [7]. The dark dimension opens up at the characteristic mass scale of the Kaluza-Klein (KK) tower,  $m_{\text{KK}} \sim \Lambda^{1/4}/\lambda$ , where physics must be described by a five-dimensional theory up to the “species scale,”  $M_{\text{UV}} \sim \lambda^{-1/3} \Lambda^{1/12} M_{\text{Pl}}^{2/3}$ , which can be regarded as the

higher dimensional Planck scale, with  $10^{-1} \lesssim \lambda \lesssim 10^{-4}$ .<sup>1</sup> The dark dimension model carries with it a rich phenomenology [10–14]. In particular, it was observed in [13] that the universal coupling of the Standard Model (SM) fields to the massive spin-2 KK excitations of the graviton in the dark dimension provides a dark-matter candidate. Complementary to the dark gravitons, it was discussed in [11] that primordial black holes with Schwarzschild radius smaller than a micron could also be good dark-matter candidates, possibly even with an interesting close relation to the dark gravitons [14].

In the dark dimension graviton (DDG) model the cosmic evolution of the hidden sector is primarily dominated by “dark-to-dark” decays, yielding a specific realization of the dynamical dark-matter framework [15]. The tower of KK

*Published by the American Physical Society under the terms of the Creative Commons Attribution 4.0 International license. Further distribution of this work must maintain attribution to the author(s) and the published article’s title, journal citation, and DOI. Funded by SCOAP<sup>3</sup>.*

<sup>1</sup>Throughout we defined the species scale in terms of the reduced Planck mass  $M_{\text{Pl}}$  rather than the Planck mass as in [8,9].

states propagating in the incredible bulk provides a rich playground for novel cosmological signals. Herein, we confront DDG predictions to experiment and demonstrate it may represent a viable alternative to the  $\Lambda$  cold-dark-matter (CDM) model.

The layout of the paper is as follows. We begin in Sec. II with a concise summary of neutrino masses, mixing, and oscillations within the context of bulk-neutrino models [16–20].<sup>2</sup> Using observational bounds on large extra dimensions we obtain constraints on the parameter space of the DDG model enriched with bulk right-handed neutrinos. In Sec. III we develop a two-step test to unambiguously distinguish DDG predictions from those of  $\Lambda$ CDM and its extensions. High-redshift postreionization cosmology with 21-cm lines allows us to perform a tomographic study of the dark ages and cosmic dawn. We show that there is a promising region of the DDG parameter space in which the modulation of redshifted 21-cm lines driven by  $KK \rightarrow \gamma\gamma$  will be within the reach of next generation experiments. Exploring in the same promising region of the parameter space, we estimate the evolution of dark matter over the age of the Universe to pin down the mass of the dark graviton today. Choosing DDG parameters from the indicated domain, we demonstrate that the sensitivity of indirect dark-matter searches targeting dwarf spheroidal galaxies are extremely competitive to detect the KK decay products in the local universe. Owing to the particular evolution of the dark-matter mass, a successful observation of both low- and high-redshift signals would allow a well-defined identification of the DDG model. In

Sec. IV we explore the global structure of the inflationary phase within the context of the dark dimension. We demonstrate that the model parameters required for a successful uniform inflation driven by a five-dimensional cosmological constant (corresponding to a flat region of the five-dimensional potential) are natural. The paper wraps up with some conclusions presented in Sec. V.

## II. CONSTRAINTS FROM NEUTRINO OSCILLATION EXPERIMENTS

We adopt the working assumption that neutrino masses originate in three five-dimensional fermion fields  $\Psi_\alpha \equiv (\psi_{\alpha L}, \psi_{\alpha R})$ , which are singlets under the SM gauge symmetries and interact on our brane with the three active left-handed neutrinos  $\nu_{\alpha L}$  in a way that conserves lepton number, where the indices  $\alpha = e, \mu, \tau$  denote the generation [16–20]. From a four-dimensional perspective, each of the singlet fermion fields can be decomposed as an infinite tower of KK states,  $\psi_{L(R)}^\kappa$ , with  $\kappa = 0, \pm 1, \dots, \pm\infty$ . The right-handed bulk states  $\psi_R^\kappa$  combine with the left-handed bulk components  $\psi_L^\kappa$  to form Dirac mass terms, which derive from the quantized internal momenta in the dark dimension. The bulk states also mix with the active left-handed neutrinos through Dirac-like mass terms. Redefining the bulk fields as  $\nu_{\alpha R}^{(0)} \equiv \psi_{\alpha R}^{(0)}$  and  $\nu_{\alpha L(R)}^{(K)} \equiv (\psi_{\alpha L(R)}^{(K)} + \psi_{\alpha L(R)}^{(-K)})/\sqrt{2}$ , after electroweak symmetry breaking the mass terms of the Lagrangian take the form

$$\begin{aligned} \mathcal{L}_{\text{mass}} &= \sum_{\alpha\beta} m_{\alpha\beta}^D \left[ \bar{\nu}_{\alpha L}^{(0)} \nu_{\beta R}^{(0)} + \sqrt{2} \sum_{K=1}^{\infty} \bar{\nu}_{\alpha L}^{(0)} \nu_{\beta R}^{(K)} \right] + \sum_{\alpha} \sum_{K=1}^{\infty} m_K \bar{\nu}_{\alpha L}^{(K)} \nu_{\alpha R}^{(K)} + \text{H.c.} \\ &= \sum_{i=1}^3 \bar{\mathbb{N}}_{iR} \mathbb{M}_i \mathbb{N}_{iL} + \text{H.c.}, \end{aligned} \quad (1)$$

where  $m_{\alpha\beta}^D$  is a Dirac mass matrix,  $m_K = K/R = Km_{\text{KK}}$ ,

$$\mathbb{N}_{iL(R)} = (\nu_i^{(0)}, \nu_i^{(1)}, \nu_i^{(2)}, \dots)_{L(R)}^T, \quad \text{and} \quad \mathbb{M}_i = \begin{pmatrix} m_i^D & 0 & 0 & 0 & \dots \\ \sqrt{2}m_i^D & 1/R & 0 & 0 & \dots \\ \sqrt{2}m_i^D & 0 & 2/R & 0 & \dots \\ \vdots & \vdots & \vdots & \vdots & \ddots \end{pmatrix}, \quad (2)$$

and where  $m_i^D$  are the elements of the diagonalized Dirac mass matrix  $= \text{diag}(m_1^D, m_2^D, m_3^D)$ . Greek indices from the

beginning of the alphabet run over the three active flavors ( $\alpha, \beta = e, \mu, \tau$ ), Roman lower case indices over the three SM families ( $i = 1, 2, 3$ ), and capital Roman indices over the KK modes ( $K = 1, 2, 3, \dots, +\infty$ ). Note that  $\psi_{\alpha L}^{(0)}$  decouples from the system. For the configuration at hand,

<sup>2</sup>Neutrino masses in relation to the swampland program were discussed in [21,22].

$$m_i^D \approx \frac{y_i \langle H \rangle}{\sqrt{R M_{UV}}}, \quad (3)$$

where  $y_i$  are the Yukawa couplings and  $\langle H \rangle$  the Higgs vacuum expectation value.

A quantity of pivotal interest is  $P(\nu_\alpha \rightarrow \nu_\beta)$ , which defines the probability of finding a neutrino of flavor  $\beta$  in a beam that was born with flavor  $\alpha$  and has traveled a distance  $L$ . Armed with the Lagrangian (1) it is straightforward to parametrize  $P(\nu_\alpha \rightarrow \nu_\beta)$  in terms of three mixing angles ( $\theta_{12}, \theta_{13}, \theta_{23}$ ), a Dirac  $CP$ -violating phase ( $\delta_{13}$ ), and the solar ( $\Delta m_{21}^2$ ) and atmospheric ( $\Delta m_{31}^2$ ) mass differences [16–20]. Short- and long-baseline experiments constrain the standard six oscillation parameters and two extra parameters taken to be  $R$  and  $m_0 \equiv m_{1(3)}^D$  for the normal hierarchy  $m_3 > m_2 > m_1 = m_0$  and (inverted hierarchy  $m_2^D > m_1^D > m_3^D = m_0$ ) [19,23]. The most recent analysis of neutrino oscillations, combining data from MINOS/MINOS+, Daya Bay, and KATRIN, gives  $R < 0.4 \mu\text{m}$ , for the normal hierarchy, and  $R < 0.2 \mu\text{m}$ , for the inverted hierarchy, both upper limits at 99% C.L. [24].<sup>3</sup> This implies that  $m_{KK} \gtrsim 2.5 \text{ eV}$ , and therefore  $\lambda \lesssim 10^{-3}$ . The associated upper limit on the compactification radius  $R$  is 2 orders of magnitude below the previously predicted maximum size of the dark dimension. The less restrictive bound is based on null results in the search for deviations from Newton's gravitational inverse-square law in the short length-scale regime [4,5].

### III. TWO-STEP TEST OF DYNAMICAL DARK GRAVITON COSMOLOGY

This section describes an overall framework for DDG model identification. We show that observations at low and high redshift from next generation experiments could be used to unequivocally identify the cosmic evolution of the incredible bulk [15]. As an illustration, we proceed here with normalization of the model parameters at high redshift to establish model predictions for the local Universe; but of course, this direction can be turned the other way around.

#### A. Probing the dark dimension with highly redshifted 21-cm line

During the emission of the cosmic microwave background (CMB) at redshift  $z_{\text{CMB}} \sim 1100$ , matter dominates the energy density of the Universe. The number density of baryons is mostly composed of neutral hydrogen atoms ( $H_1$ ), together with a smaller Helium (He) component,  $x_{\text{He}} = n_{\text{He}}/n_{H_1} \simeq 1/13$ , and a small percentage of free protons and electrons,  $x_e = n_e/n_{H_1} = n_p/n_{H_1}$ , which varies

<sup>3</sup>A point worth noting at this juncture is that in the presence of bulk masses, right-handed neutrinos propagating in the dark dimension can induce electron-neutrino appearance effects [25]. These effects can help relax the bound on  $R$  and have the potential to address the LSND  $\bar{\nu}_\mu \rightarrow \bar{\nu}_e$  anomaly [26].

from about 20% at  $z_{\text{CMB}}$  to roughly  $2 \times 10^{-4}$  at  $z \sim 20$  [27]. After the gas thermally decouples from the photon temperature at  $z_{\text{dec}} \sim 150$ , most of the hydrogen gas is in its ground state, whose degeneracy is only broken by the hyperfine splitting of the spin-0 singlet and spin-1 triplet. In the rest frame of the gas, the energy gap between these two spin states is  $E_{21} = 5.9 \times 10^{-6} \text{ eV} \simeq 2\pi/21 \text{ cm}$ , corresponding to a  $\nu_{21} = 1.4 \text{ GHz}$  spectral line. The relative number density of the two spin levels,  $n_1/n_0 = 3e^{-E_{21}/T_s}$ , defines the spin temperature  $T_s$ , where the factor of 3 comes from the degeneracy of the triplet excited state. Because of the 21-cm transitions, for a given redshift  $z < z_{\text{dec}}$ , a shell of  $H_1$  can act as a detector of the background photons [28]. The observable is the 21-cm brightness temperature relative to the photon background

$$T_{21}(z) \simeq 27 \text{ mK } x_{H_1}(z) \left( \frac{0.15}{\Omega_m h^2} \right)^{1/2} \left( \frac{1+z}{10} \right)^{1/2} \times \left( \frac{\Omega_b h^2}{0.02} \right) \left( 1 - \frac{T_\gamma(z)}{T_s(z)} \right), \quad (4)$$

where  $\Omega_m$  and  $\Omega_b$  are the present day values of the non-relativistic matter density and baryon energy density as a fraction of the critical density, and where  $h$  is the Hubble constant in units of 100 km/s/Mpc [29]. Note that if the photon temperature exceeds the spin temperature ( $T_{21} < 0$ ) there will be net absorption and in the opposite case ( $T_{21} > 0$ ) net emission. For  $\Lambda\text{CDM}$ ,  $T_\gamma$  is given by the CMB thermal radiation, with temperature  $T_{\text{CMB}}(z) = 2.725 \text{ K}(1+z)$ .

From the dark ages ( $1100 \lesssim z \lesssim 30$ ) to cosmic dawn ( $30 \lesssim z \lesssim 15$ ) and the subsequent epoch of reionization, the evolution of  $T_{21}$  can be schematically described by five distinctive regimes: (i) For  $z_{\text{dec}} < z < z_{\text{CMB}}$ , the non-negligible number of free electrons couples the gas to radiation,  $T_\gamma = T_{\text{gas}} = T_s$ , and there is no 21-cm signal because  $T_{21} = 0$ . For  $z < z_{\text{dec}}$ , the gas cools down more rapidly than CMB radiation, but the gas temperature has a minimum value set by its primordial heating due to Thomson scattering, and so  $T_{\text{gas}}(z) = T_{\text{CMB}}(z)(1+z)/(1+z_{\text{dec}})$ . (ii) For  $30 \lesssim z < z_{\text{dec}}$ , gas collisions are efficient enough to couple the spin and gas temperatures, i.e.,  $T_s \simeq T_{\text{gas}}$ . This means  $T_{21} < 0$ , and therefore an absorption signal is expected during the dark ages. (iii) At  $z \simeq 30$  the gas becomes so rarified that the collision rate becomes too low to enforce  $T_s \simeq T_{\text{gas}}$ , and the 21-cm signal is again suppressed  $T_{21} \simeq 0$  because  $T_s \simeq T_\gamma$ . (iv) At cosmic dawn  $z \lesssim 30$ , the first stars fired up, making the Lyman- $\alpha$  coupling strong, and thereby the spin temperature is expected to be coupled to the gas kinetic temperature, i.e.,  $T_{\text{gas}} \approx T_s$ . Again  $T_{21} < 0$ , implying an absorption signal. (v) During the epoch of reionization the gas gets reheated by astrophysical radiation yielding  $T_s \simeq T_{\text{gas}} > T_\gamma$ , so that  $T_{21}$  turns positive and one has an emission signal from the regions that are not fully ionized.

Eventually all gas gets ionized until the fraction of neutral hydrogen vanishes and the signal switches off again.

The experiment to detect the global epoch of reionization signature (EDGES) recorded the first measurement of the global 21-cm spectrum. The data are consistent with an absorption profile at  $z \sim 15$ –20, with a minimum at  $z_E = 17.2$  where  $T_{21}(z_E) = -500^{+200}_{-500}$  mK at 99% C.L., including estimates of systematic uncertainties [30]. Using (4) with  $x_{H_I} \simeq 1$  the EDGES observation implies  $T_{\text{gas}} \simeq T_s(z_E) < 3.3$  K, wherefore in tension with  $\Lambda\text{CDM}$  that predicts the minimum gas temperature to be  $T_{\text{gas}}^{\Lambda\text{CDM}}(z_E) \simeq 6$  K.<sup>4</sup>

The EDGES 21-cm signal severely constrains new physics processes which are capable of heating up the intergalactic medium prior to the reionization time, e.g., via energy injection from annihilation [33] or decaying [34–36] dark matter. For sub-MeV dark matter, EDGES bounds on the partial decay width into two photons are stronger than CMB-based limits [37] by 1 to 2 orders of magnitude.

We now turn to investigate how the EDGES bound impacts the allowed parameter space of the DDG model. We begin by considering a tower of equally spaced dark gravitons, indexed by an integer  $l$ , and with mass  $m_l = l m_{\text{KK}}$ . The partial decay width of KK graviton  $l$  to SM fields is found to be

$$\Gamma_{\text{SM}}^l = \frac{\tilde{\lambda}^2 m_{\text{KK}}^3 l^3}{80\pi M_{\text{Pl}}^2}, \quad (5)$$

where  $\tilde{\lambda}$  takes into account all the available decay channels and is a function of time [38].

The cosmic evolution of the dark sector is mostly driven by “dark-to-dark” decay processes, which regulate the decay of KK gravitons within the dark tower [13]. In the absence of isometries in the dark dimension, which is the common expectation, the KK momentum of the dark tower is not conserved. This means that a dark graviton of KK quantum  $n$  can decay to two other ones, with quantum numbers  $n_1$  and  $n_2$ . If the KK quantum violation can go up to  $\delta n$ , the number of available channels is roughly  $l\delta n$ . In addition, because the decay is almost at threshold, the phase space factor is roughly the velocity of decay products,  $v_{\text{r.m.s.}} \sim \sqrt{m_{\text{KK}}\delta n/m_l}$ . Putting all this together we obtain the total decay width,

$$\begin{aligned} \Gamma_{\text{tot}}^l &\sim \sum_{l' < l} \sum_{0 < l'' < l-l'} \Gamma_{l'l''}^l \sim \beta^2 \frac{m_l^3}{M_{\text{Pl}}^2} \times \frac{m_l}{m_{\text{KK}}} \delta n \\ &\times \sqrt{\frac{m_{\text{KK}}\delta n}{m_l}} \sim \beta^2 \delta n^{3/2} \frac{m_l^{7/2}}{M_{\text{Pl}}^2 m_{\text{KK}}^{1/2}}, \end{aligned} \quad (6)$$

<sup>4</sup>We note in passing that this interpretation has been called into question in [31], and it is in tension with the SARAS3 data [32].

where  $\beta$  parametrizes our ignorance of decays in the dark dimension [13].

We further follow [13] to estimate the time evolution of the dark-matter mass and assume that for times larger than  $1/\Gamma_{\text{tot}}^l$  dark matter which is heavier than the corresponding  $m_l$  has already decayed, yielding

$$m_l \sim \left( \frac{M_{\text{Pl}}^4 m_{\text{KK}}}{\beta^4 \delta n^3} \right)^{1/7} t^{-2/7}, \quad (7)$$

where  $t$  indicates the time elapsed since the big bang.

All in all, the recombination history of the Universe would be modified by dark gravitons decaying into SM fields, as these visible fields inject energy into the (pre-recombination) photon-baryon plasma and (postrecombination) gas and background radiation. The energy injection would increase the ionization of the gas, the atomic excitation of the gas, and the plasma/gas heating. These three processes would therefore increase the residual ionization fraction ( $x_e$ ) and baryon temperature after recombination. Consistency with CMB anisotropies requires  $\Gamma_{\gamma\gamma}^l < 5 \times 10^{-25} \text{ s}^{-1}$  between the last scattering surface and reionization [37]. In our calculations we set  $\lambda \sim 10^{-3}$  to accommodate neutrino masses with three generations of massless bulk fermions. Taking  $\tilde{\lambda} = 1$  to set out the decay into photons we can use (5) to find that the CMB requirement is satisfied for  $l \lesssim 10^8$  at the time  $t_{\text{MR}} \sim 6 \times 10^4$  yr of matter-radiation equality. In other words, by setting  $\tilde{\lambda} \sim 1$  and  $m_l(t_{\text{MR}}) \lesssim 1$  MeV we find that the evolution of  $m_l$  with cosmic time given in (7) is such that at the last scattering surface the dominant KK state in the dynamical dark-matter ensemble has the correct decay width to accommodate the CMB constraints. This is shown in Fig. 1 where we display  $\Gamma_{\gamma\gamma}^l(t)$  normalized to  $m_l(t_{\text{MR}}) = 1$  MeV.

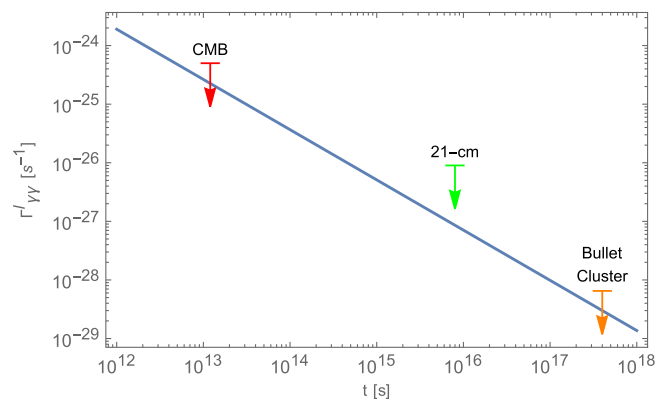


FIG. 1.  $\Gamma_{\gamma\gamma}^l$  as a function of the age of the Universe. The curve is normalized to a dark-matter mass of 1 MeV at the time of matter-radiation equality. Bounds on the partial decay width of dark matter decaying into two photons from CMB anisotropies [37], 21-cm absorption line detected by EDGES [35,36], and the bullet cluster [39] are shown for comparison. The age of the Universe is taken to be 13 Gyr [40].



As can be seen in Fig. 1, for the selected set of fiducial parameters, DDG predictions from KK decay into SM fields saturate current upper limits placed by EDGES data on  $\Gamma_{\gamma\gamma}^l$  [35,36]. This means that for this particular region of the parameter space, DDG predictions are within reach of next generation experiments. In particular, interferometric experiments like the upcoming square kilometre array (SKA) will have the sensitivity to make high-resolution spectra of high-redshift radio sources to probe the 21-cm signal at Cosmic Dawn [41]. The photon emission from KK graviton decay could be distinguished from simple X-ray heating by (i) occurring before the epoch of galaxy formation and (ii) by depositing energy more uniformly than would be expected from galaxy clustering [42]. The lunar FARSIDE array will measure the dark ages global 21-cm signal at redshifts  $35 < z < 200$ , extending the sensitivity down 2 orders of magnitude below frequency bands accessible to ground-based radio astronomy [43]. Thus, FARSIDE will provide an important test, both of KK decays into SM fields and of the ideas discussed in this paper.

Once the free parameters of the model have been adjusted to accommodate 21-cm data, we can use (5) and (7) to make predictions that can be confronted with observations in the local Universe. For example, for  $m_l(t_{\text{MR}}) \sim 1$  MeV, (7) leads to  $m_l(t_{\text{today}}) \sim 50$  keV. Now, we have seen that dark-matter decay gives the daughter particles a velocity kick. Self-gravitating dark-matter halos that have a virial velocity smaller than this velocity kick may be disrupted by these particle decays. Combined cosmological enlarged simulations of decaying dark matter with a model of the Milky Way satellite population rule out nonrelativistic kick speeds  $\gtrsim 10^{-4}$  for a dark-matter lifetime  $\tau_{\text{DM}} \lesssim 29$  Gyr at 95% C.L. [44]. However, N-body simulations of isolated dark-matter halos seem to indicate that if  $\tau_{\text{DM}} \gtrsim 60$  Gyr and the kick speed  $\lesssim 10^{-2}$  then the halos are essentially unchanged [45]. Setting  $\delta n \sim 1$  [46] and taking  $\beta \sim 635$  to match our normalization [ $l \sim 10^8$  at  $t_{\text{MR}}$ ; see (7)], we obtain  $\tau_{m_l(\text{today})} \sim 68$  Gyr, and so the kick velocity of the decay products,  $v_{\text{r.m.s.}} \sim 5 \times 10^{-3}$ , is consistent with the mass concentration of self-gravitating dark-matter halos.<sup>5</sup>

### B. Indirect dark-matter searches on dwarf spheroidals and cluster of galaxies

In line with our stated plan, we now adopt the parameter space within reach of 21-cm data as a benchmark, and we confront predictions of the DDG model with null results of indirect dark-matter searches targeting dwarf spheroidal and cluster of galaxies. These astrophysical environments

are the best promising targets to search for signals of decaying dark matter in the local Universe, because they have a low content of gas and dust, as well as a high mass-to-light ratio, and they are free of astrophysical photon-emitting sources. Besides, dwarf spheroidals are also relatively nearby, and many lie far enough from the Galactic plane to have low Galactic foreground.

There are restrictive bounds on  $\Gamma_{\gamma\gamma}^l$  from null results of indirect dark-matter searches targeting dwarf spheroidals and cluster of galaxies. In particular, null results from searches by the NuSTAR Collaboration in the direction of the bullet cluster can be translated into an upper limit  $\Gamma_{\gamma\gamma}^{\text{CDM}} < 10^{-28} \text{ s}^{-1}$  for dark-matter masses in the 10 to 50 keV range [39].

Analyzing the optimal region of the phase space explored in the previous section, we find that for our choice of parameters, DDG predictions saturate the bullet cluster bound (see Fig. 1), suggesting that indirect detection dark-matter experiments are extremely competitive to detect the KK decay products in the local Universe.

### C. Recapitulation

We presented a two-step test of the DDG model. We have shown that for  $\tilde{\lambda} \sim 1$ ,  $\delta n \sim 1$ ,  $\beta \sim 635$ , and  $m_l(t_{\text{MR}}) \sim 1$  MeV the cosmic evolution of the dynamical KK ensemble predicts via (7) a dominant particle mass of  $\sim 900$  keV at CMB, of  $\sim 500$  keV in the dark ages, of  $\sim 150$  keV at cosmic dawn, and of  $\sim 50$  keV in the local Universe. This is in sharp contrast to typical dark-matter decay scenarios with one unstable particle (such as sterile neutrinos [47]). For our fiducial parameters, the corresponding decay widths of  $\text{KK} \rightarrow \gamma\gamma$  will be within reach of next generation experiments probing the low- and high-redshift Universe. Thus, a combination of positive results in future observational campaigns can be used to pinpoint the DDG model.

### IV. HIGUCHI BOUND AND THE SHAPE OF INFLATION

In de Sitter (dS) spacetime (of radius  $1/H$ ) there exists an absolute minimum for a field of spin-2 and mass  $m_2$  set by the Higuchi bound

$$m_2^2 \geq 2H^2, \quad (8)$$

where  $H = \Lambda^2/M_{\text{Pl}} \sim 10^{-34} \text{ eV}$  is the Hubble parameter [48]. If the bound is violated the massive spin-2 field contains helicity modes with negative norm, which are in conflict with unitarity. Hence, if we define the “size” of the extra dimensions by the inverse mass of the lightest KK excitation of the graviton, the Higuchi bound forbids any compactification in which the extra dimensions are larger than and  $\mathcal{O}(1)$  factor times  $1/H$  [49].

Now, since  $H \ll m_{\text{KK}} \sim \Lambda^{1/4}/\lambda$ , the Higuchi bound is inordinately satisfied by the DDG construct today. However, the Higuchi bound forbids the presence of the

<sup>5</sup>Since the model is a realization of dynamical dark matter [15], a dedicated simulation should be done to ensure full compatibility with the evolution of structure formation.

DDG tower over a dS background within the mass range  $0 \leq m_I^2 \leq 2H_I^2$ , which would imply that KK excitations could not be excited during inflation. Indeed, the inflation scale is given by  $M_I = \Lambda_I^{1/4} = 3^{1/4} \sqrt{M_*^I H_I}$ , where  $M_*^I = M_{\text{Pl}}/\sqrt{N_I}$  is the strength of gravity at the inflation scale, with  $N_I = M_*^I/m_{\text{KK}}$  the number of species with masses below the inflation scale. Now, using the standard formulas from slow roll single field inflation and input from the experiment for the amplitude of density perturbations, the Hubble factor during inflation is found to be  $H_I \sim 10^{-4} \sqrt{r} M_*^I$ , with  $r$  the tensor to scalar ratio of primordial gravitational waves [50].<sup>6</sup> If the radion is fixed during inflation (in 4 dimensions) the Higuchi bound gives  $H_I \lesssim m_{\text{KK}} \lesssim \text{eV}$ , implying  $M_I \lesssim 100 \text{ GeV}$ . To confront this obstacle we adopt the working assumption that the Universe undergoes a period of inflation in which the radius of the dark dimension expanded exponentially fast, from the species length up to the micron scale.<sup>7</sup>

The core idea behind the inflationary phase takes after the procedure adopted in string theories with large internal dimensions and TeV-scale gravity [53–55]. The higher-dimensional metric is given by

$$ds_5^2 = a_5^2(-d\eta^2 + d\vec{x}^2 + r_0^2 dy^2), \quad (9)$$

where  $\eta$  is the conformal time,  $a_5 = -1/(H\eta)$ ,  $\vec{x}$  denotes the three uncompactified dimensions, and  $r_0 \sim 1/M_{\text{UV}}$  is the radius of the dark dimension  $y$  at the beginning of the inflationary phase. The four-dimensional decomposition in the Einstein frame is found to be

$$ds_5^2 = \frac{1}{R} ds_4^2 + R^2 dy^2, \quad (10)$$

where  $ds_4^2 = a_4^2(-d\eta^2 + d^2\vec{x})$ . Comparing (9) and (10) we arrive at  $a_4/\sqrt{R} = R$ . After inflation of  $N$   $e$ -folds, where the scale factor was expanded by  $a_5 = e^N$ , the radius becomes  $R = e^N$ . We want  $r_0$  to grow fast up to the micron scale. This requires 42  $e$ -folds. Now, if  $R$  expands  $N$   $e$ -folds, then the four-dimensional space would expand  $3N/2$   $e$ -folds as a result of a uniform five-dimensional inflation. Hence, 42  $e$ -folds in  $R$  implies 63  $e$ -folds in the noncompact space to successfully address the horizon problem [56,57]. We can now obtain an upper limit on the scale of inflation by noting that for  $m_{\text{KK}} \sim 1 \text{ eV}$ , we have  $M_*^I \sim 2 \times 10^9 \text{ GeV}$ , and so  $M_I = 10^{-2} M_*^I r^{1/4} \lesssim 8 \times 10^6 \text{ GeV}$ .

The inflaton mass  $m_\phi$  is model dependent, and we will take it as a free parameter. To produce matter on the brane it is sufficient to introduce a Yukawa-like coupling  $y$  of the inflaton to brane fermions, and so the decay width is

$$\Gamma_{f\bar{f}}^\phi \sim y^2 m_\phi \frac{m_{\text{KK}}}{M_{\text{UV}}}, \quad (11)$$

where the last factor  $m_{\text{KK}}/M_{\text{UV}}$  comes from the volume suppression. This suppression is similar to the one in (3) for the case of bulk right-handed neutrinos. The decay width into gravitons is Planck suppressed, and we have to carry out only one sum up to  $l$  because  $\delta n \sim 1$ . By dimensional analysis,

$$\Gamma_{\text{grav}}^\phi \sim \frac{m_\phi^3}{M_{\text{Pl}}^2} \times \frac{m_\phi}{m_{\text{KK}}} \times \delta n \sim \frac{m_\phi^4}{M_{\text{UV}}^3}. \quad (12)$$

Comparing the decay rate of SM fields (11) to that of gravitons (12) we impose

$$\left( \Gamma_{f\bar{f}}^\phi \sim \frac{m_{\text{KK}}}{M_{\text{UV}}} m_\phi \right) > \left( \Gamma_{\text{grav}}^\phi \sim \frac{m_\phi^4}{M_{\text{UV}}^3} \right), \quad (13)$$

where we have taken  $y \sim 1$ . All in all, (13) gives a bound for the mass of the inflaton  $m_\phi < 1 \text{ TeV}$ . The suppressed decay into gravitons ensures that the upper limit on the number of “equivalent” light neutrino species ( $\Delta N_{\text{eff}} < 0.214$  at 95% C.L. [40]) present in the era before recombination is satisfied [58]. The KK decomposition of the five-dimensional metric gives rise to a tower of massive physical states of spin two, while the radion is reduced only to the four-dimensional zero mode. This is to be contrasted with the TeV-scale model advocated in [59], in which the inflaton is a field localized on the brane. However, in both cases the inflaton decays reheat predominantly brane states while not producing significant numbers of gravitons.

## V. CONCLUSIONS

In the first part of this paper we generalized studies of large-extra-dimension models originally set up to interpret the smallness of neutrino masses by postulating that right-handed neutrinos, unlike SM fields, do propagate in the bulk [16–20]. We showed that when interpreted in the context of the dark dimension, neutrino oscillation data constrain the characteristic mass scale of the KK tower:  $m_{\text{KK}} > 2.5 \text{ eV}$  at the 99% C.L. This constraint represents a 2 order of magnitude improvement over the bound on short-range deviations from Newton’s gravitational law [4,5].

In the second part of the paper we proposed a method to test a particular realization of the incredible bulk of dynamical dark matter [15] in which the ensemble of KK modes originates in a compact (dark) dimension with characteristic length scale in the micron range [7,13]. Since the cosmic evolution of the dark sector is driven by dark-to-dark intraensemble decays, the model is particularly challenging to probe. We developed a two-step process test to unambiguously distinguish predictions of the dark dimension gravitons from those of the  $\Lambda$ CDM model.

<sup>6</sup>The latest CMB observations of BICEP/Keck, combined with those of WMAP and the Planck mission, place a strong upper bound  $r \leq 0.036$  (at 95% C.L.) [51].

<sup>7</sup>Other aspects of inflation and higher spin states in relation to the Higuchi bound were discussed in [52].

Measurements of redshifted 21-cm lines allow us to perform a tomographic study of the dark ages and cosmic dawn to search for the photon emission from KK graviton decay. We showed that the changes induced by  $KK \rightarrow \gamma\gamma$  on the 21-cm signal could be within the reach of next generation experiments and can be used to make the model fully predictable. In particular, we can estimate the evolution of the dark graviton mass over the age of the Universe to pin down its value today. We demonstrated that the sensitivity of indirect dark matter searches targeting dwarf spheroidals and cluster of galaxies is extremely competitive to detect the KK decay products in the local Universe.

In the last part of this paper we examined the global structure of the inflationary phase within the context of the dark dimension. We have shown that the model parameters required for a successful uniform inflation driven by a five-dimensional cosmological constant (corresponding to a flat region of the five-dimensional potential) are natural.

In closing, we comment on how to make use of the DDG model to try resolving an emerging tension between high- and low-redshift observations. The growth of cosmic structure is parametrized by

$$S_8 = \sigma_8 \left( \frac{\Omega_m}{0.3} \right)^{0.5}, \quad (14)$$

where  $\sigma_8$  measures the r.m.s. amplitude of the clustering of matter; more accurately,

$$\sigma_8^2 = \frac{1}{2\pi^2} \int \frac{dk}{k} W^2(kR) k^3 P(k), \quad (15)$$

where  $P(k)$  is the linear matter power spectrum at  $z = 0$  and  $W(kR)$  is a top-hat filter describing a sphere (in Fourier space) with a (historically chosen [60]) radius  $R = 8 \text{ Mpc}/h$ , and where  $h$  is the dimensionless Hubble constant. Over the past few years, a tension has emerged between  $S_8$  as inferred by constraining  $\Lambda$ CDM parameters with CMB data ( $S_8 = 0.834 \pm 0.017$ ) [40] and as measured from late-Universe datasets; e.g., KIDS weak lensing surveys ( $S_8 = 0.759 \pm 0.024$ ) [61] and DES combined analysis of the clustering of foreground galaxies and lensing of background galaxies ( $S_8 = 0.776 \pm 0.017$ ) [62].

It was first proposed in [63] that the  $S_8$  tension can be relaxed if a fraction of CDM is unstable and decays into invisible massless particles. These invisible particles, which interact only via gravity with the visible SM sector, are generally referred to as dark radiation (DR). It is evident that a reduction of  $\Omega_m$  in (14) can help accommodate the observed discrepancy in  $S_8$ . However, as the decay into DR increases depleting the abundance of CDM at late times, the gravitational lensing effect due to the evolving large-scale structure is reduced. To accommodate the  $S_8$  mismatch a

high decay rate of  $CDM \rightarrow DR$  is required and therefore the lensing effect is markedly suppressed. This in turn implies that there is less transfer of power on the CMB spectra with respect to the reference  $\Lambda$ CDM. The decay  $CDM \rightarrow DR$  is well-constrained by high- $\ell$  CMB data because of the reduced small-scale anisotropies from the massless decay products. In particular, data from the Planck mission lead to an upper bound on the decay rate,  $\Gamma_{DR}^{CDM} < 10^{-19} \text{ s}^{-1}$  at 95% C.L. [64,65], which is insufficient to accommodate the  $S_8$  tension.

Resolving the  $S_8$  tension requires decreasing the amplitude of matter fluctuations on scales  $k \sim 0.5 \text{ h/Mpc}$  [66]. This can be achieved with decaying CDM into one massive warm dark matter (WDM) particle and one massless particle, both interacting only through gravitation with SM fields. A critical difference from the previous scenario is that the massive daughter particle could be born relativistic at  $z_{\text{decay}}$ , when the expansion rate is given by  $H(z_{\text{decay}})$ , but behave like CDM as the Universe evolves. The relativistic massive decay product would suppress the formation of cosmic structure, because at production it free streams with finite kick velocity and can escape from the gravitational potential wells surrounding matter over densities. The decay of  $CDM \rightarrow DR + WDM$  produces a change in both  $\sigma_8$  and  $\Omega_m$  and can accommodate the  $S_8$  tension if  $\Gamma_{DR+WDM}^{CDM} \sim 6 \times 10^{-19} \text{ s}^{-1}$  [66]. This is because the WDM component partially contributes to the matter energy density slowing down the lensing suppression of the CMB [64]. Note that such a decay width corresponds to a lifetime  $\tau_{DM} \sim 53 \text{ Gyr}$ . More recent analyses suggest that the parameter space that can accommodate the  $S_8$  tension favored by current data points to  $\tau_{DM} \sim 100 \text{ Gyr}$  and  $v_{r.m.s.} \sim 10^{-3}$  [67–69]. While the fiducial values entertained in the previous section ( $\tau_{m/(today)} \sim 68 \text{ Gyr}$  and  $v_{r.m.s.} \sim 5 \times 10^{-3}$ ) are in the ballpark and it is tempting to investigate whether the DDG model can resolve the  $S_8$ , we note that any scan of the DDG parameter space to try to accommodate the  $S_8$  requirements would be in need of a full-scale numerical simulation considering the evolution of the intraensemble KK decays throughout the history of the Universe. Such an interesting task is beyond the scope of the present study.

## ACKNOWLEDGMENTS

We have greatly benefited from discussions with Nima Arkani-Hamed, Miguel Montero, and Cumrun Vafa. The work of L. A. A. is supported by the U.S. National Science Foundation (NSF Grant No. PHY-2112527). The work of D. L. is supported by the Origins Excellence Cluster and by the German-Israel-Project (DIP) on Holography and the Swampland.



- [1] H. Ooguri and C. Vafa, On the geometry of the string landscape and the swampland, *Nucl. Phys.* **B766**, 21 (2007).
- [2] D. Lüster, E. Palti, and C. Vafa, AdS and the swampland, *Phys. Lett. B* **797**, 134867 (2019).
- [3] C. Vafa, The string landscape and the swampland, [arXiv: hep-th/0509212](#).
- [4] D. J. Kapner, T. S. Cook, E. G. Adelberger, J. H. Gundlach, B. R. Heckel, C. D. Hoyle, and H. E. Swanson, Tests of the Gravitational Inverse-Square Law Below the Dark-Energy Length Scale, *Phys. Rev. Lett.* **98**, 021101 (2007).
- [5] J. G. Lee, E. G. Adelberger, T. S. Cook, S. M. Fleischer, and B. R. Heckel, New Test of the Gravitational  $1/r^2$  Law at Separations Down to 52  $\mu\text{m}$ , *Phys. Rev. Lett.* **124**, 101101 (2020).
- [6] S. Hannestad and G. G. Raffelt, Supernova and neutron star limits on large extra dimensions reexamined, *Phys. Rev. D* **67**, 125008 (2003); **69**, 029901(E) (2004).
- [7] M. Montero, C. Vafa, and I. Valenzuela, The dark dimension and the swampland, *J. High Energy Phys.* **02** (2023) 022.
- [8] G. Dvali, Black holes and large  $N$  species solution to the hierarchy problem, *Fortschr. Phys.* **58**, 528 (2010).
- [9] G. Dvali and M. Redi, Black hole bound on the number of species and quantum gravity at LHC, *Phys. Rev. D* **77**, 045027 (2008).
- [10] L. A. Anchordoqui, The dark dimension, the Swampland, and the origin of cosmic rays beyond the GZK barrier, *Phys. Rev. D* **106**, 116022 (2022).
- [11] L. Anchordoqui, I. Antoniadis, and D. Lüster, The dark dimension, the swampland, and the dark matter fraction composed of primordial black holes, *Phys. Rev. D* **106**, 086001 (2022).
- [12] R. Blumenhagen, M. Brinkmann, and A. Makridou, The dark dimension in a warped throat, *Phys. Lett. B* **838**, 137699 (2023).
- [13] E. Gonzalo, M. Montero, G. Obied, and C. Vafa, Dark dimension gravitons as dark matter, [arXiv:2209.09249](#).
- [14] L. Anchordoqui, I. Antoniadis, and D. Lüster, The dark universe: Primordial black hole  $\rightleftharpoons$  dark graviton gas connection, *Phys. Lett. B* **840**, 137844 (2023).
- [15] K. R. Dienes and B. Thomas, Dynamical dark matter: I. Theoretical overview, *Phys. Rev. D* **85**, 083523 (2012).
- [16] K. R. Dienes, E. Dudas, and T. Gherghetta, Neutrino oscillations without neutrino masses or heavy mass scales: A Higher dimensional seesaw mechanism, *Nucl. Phys.* **B557**, 25 (1999).
- [17] N. Arkani-Hamed, S. Dimopoulos, G. R. Dvali, and J. March-Russell, Neutrino masses from large extra dimensions, *Phys. Rev. D* **65**, 024032 (2001).
- [18] G. R. Dvali and A. Y. Smirnov, Probing large extra dimensions with neutrinos, *Nucl. Phys.* **B563**, 63 (1999).
- [19] H. Davoudiasl, P. Langacker, and M. Perelstein, Constraints on large extra dimensions from neutrino oscillation experiments, *Phys. Rev. D* **65**, 105015 (2002).
- [20] I. Antoniadis, E. Kiritsis, J. Rizos, and T. N. Tomaras, D-branes and the standard model, *Nucl. Phys.* **B660**, 81 (2003).
- [21] L. E. Ibanez, V. Martin-Lozano, and I. Valenzuela, Constraining neutrino masses, the cosmological constant and BSM physics from the weak gravity conjecture, *J. High Energy Phys.* **11** (2017) 066.
- [22] E. Gonzalo, L. E. Ibáñez, and I. Valenzuela, Swampland constraints on neutrino masses, *J. High Energy Phys.* **02** (2022) 088.
- [23] P. A. N. Machado, H. Nunokawa, and R. Zukanovich Funchal, Testing for large extra dimensions with neutrino oscillations, *Phys. Rev. D* **84**, 013003 (2011).
- [24] D. V. Forero, C. Giunti, C. A. Ternes, and O. Tyagi, Large extra dimensions and neutrino experiments, *Phys. Rev. D* **106**, 035027 (2022).
- [25] M. Carena, Y. Y. Li, C. S. Machado, P. A. N. Machado, and C. E. M. Wagner, Neutrinos in large extra dimensions and short-baseline  $\nu_e$  appearance, *Phys. Rev. D* **96**, 095014 (2017).
- [26] A. Aguilar *et al.* (LSND Collaboration), Evidence for neutrino oscillations from the observation of  $\bar{\nu}_e$  appearance in a  $\bar{\nu}_\mu$  beam, *Phys. Rev. D* **64**, 112007 (2001).
- [27] Y. Ali-Haïmoud and C. M. Hirata, Ultrafast effective multi-level atom method for primordial hydrogen recombination, *Phys. Rev. D* **82**, 063521 (2010).
- [28] J. R. Pritchard and A. Loeb, 21-cm cosmology, *Rep. Prog. Phys.* **75**, 086901 (2012).
- [29] M. Zaldarriaga, S. R. Furlanetto, and L. Hernquist, 21 Centimeter fluctuations from cosmic gas at high redshifts, *Astrophys. J.* **608**, 622 (2004).
- [30] J. D. Bowman, A. E. E. Rogers, R. A. Monsalve, T. J. Mozdzen, and N. Mahesh, An absorption profile centred at 78 megahertz in the sky-averaged spectrum, *Nature (London)* **555**, 67 (2018).
- [31] R. Hills, G. Kulkarni, P. D. Meerburg, and E. Puchwein, Concerns about modelling of the EDGES data, *Nature (London)* **564**, E32 (2018).
- [32] H. T. J. Bevens, A. Fialkov, E. d. Acedo, W. J. Handley, S. Singh, R. Subrahmanyam, and R. Barkana, Astrophysical constraints from the SARAS 3 non-detection of the cosmic dawn sky-averaged 21-cm signal, *Nat. Astron.* **6**, 1473 (2022).
- [33] G. D'Amico, P. Panci, and A. Strumia, Bounds on Dark Matter Annihilations from 21 cm Data, *Phys. Rev. Lett.* **121**, 011103 (2018).
- [34] V. Poulin, J. Lesgourgues, and P. D. Serpico, Cosmological constraints on exotic injection of electromagnetic energy, *J. Cosmol. Astropart. Phys.* **03** (2017) 043.
- [35] S. Clark, B. Dutta, Y. Gao, Y. Z. Ma, and L. E. Strigari, 21 cm limits on decaying dark matter and primordial black holes, *Phys. Rev. D* **98**, 043006 (2018).
- [36] H. Liu and T. R. Slatyer, Implications of a 21-cm signal for dark matter annihilation and decay, *Phys. Rev. D* **98**, 023501 (2018).
- [37] T. R. Slatyer and C. L. Wu, General constraints on dark matter decay from the cosmic microwave background, *Phys. Rev. D* **95**, 023010 (2017).
- [38] L. J. Hall and D. Tucker-Smith, Cosmological constraints on theories with large extra dimensions, *Phys. Rev. D* **60**, 085008 (1999).
- [39] S. Riemer-Sørensen, D. Wik, G. Madejski, S. Molendi, F. Gastaldello, F. A. Harrison, W. W. Craig, C. J. Hailey, S. E. Boggs, F. E. Christensen *et al.*, Dark matter line emission constraints from NuSTAR observations of the Bullet Cluster, *Astrophys. J.* **810**, 48 (2015).



- [40] N. Aghanim *et al.* (Planck Collaboration), Planck 2018 results VI: Cosmological parameters, *Astron. Astrophys.* **641**, A6 (2020); **652**, C4(E) (2021).
- [41] A. Weltman, P. Bull, S. Camera, K. Kelley, H. Padmanabhan, J. Pritchard, A. Raccanelli, S. Riemer-Sørensen, L. Shao, S. Andrianomena *et al.*, Fundamental physics with the Square Kilometre Array, *Pub. Astron. Soc. Aust.* **37**, e002 (2020).
- [42] M. Valdes, A. Ferrara, M. Mapelli, and E. Ripamonti, Constraining DM through 21 cm observations, *Mon. Not. R. Astron. Soc.* **377**, 245 (2007).
- [43] J. Burns, G. Hallinan, T.C. Chang, M. Anderson, J. Bowman, R. Bradley, S. Furlanetto, A. Hegedus, J. Kasper, J. Kocz *et al.*, A lunar farside low radio frequency array for dark ages 21-cm cosmology, [arXiv:2103.08623](https://arxiv.org/abs/2103.08623).
- [44] S. Mau *et al.* (DES Collaboration), Milky way satellite census IV: Constraints on decaying dark matter from observations of Milky Way satellite galaxies, *Astrophys. J.* **932**, 128 (2022).
- [45] A. H. G. Peter, C. E. Moody, and M. Kamionkowski, Dark-matter decays and self-gravitating halos, *Phys. Rev. D* **81**, 103501 (2010).
- [46] C. Vafa (private communication).
- [47] K. N. Abazajian, Sterile neutrinos in cosmology, *Phys. Rep.* **711–712**, 1 (2017).
- [48] A. Higuchi, Forbidden mass range for spin-2 field theory in De Sitter space-time, *Nucl. Phys.* **B282**, 397 (1987).
- [49] M. Kleban, M. Mirbabayi, and M. Porrati, Effective planck mass and the scale of inflation, *J. Cosmol. Astropart. Phys.* **01** (2016) 017.
- [50] I. Antoniadis and S. P. Patil, The effective planck mass and the scale of inflation, *Eur. Phys. J. C* **75**, 182 (2015).
- [51] P. A. R. Ade *et al.* (BICEP/Keck Collaboration), Improved Constraints on Primordial Gravitational Waves using Planck, WMAP, and BICEP/Keck Observations through the 2018 Observing Season, *Phys. Rev. Lett.* **127**, 151301 (2021).
- [52] M. Scalisi, Inflation, higher spins and the swampland, *Phys. Lett. B* **808**, 135683 (2020).
- [53] I. Antoniadis, N. Arkani-Hamed, S. Dimopoulos, and G. R. Dvali, New dimensions at a millimeter to a Fermi and superstrings at a TeV, *Phys. Lett. B* **436**, 257 (1998).
- [54] N. Arkani-Hamed, S. Dimopoulos, N. Kaloper, and J. March-Russell, Rapid asymmetric inflation and early cosmology in theories with submillimeter dimensions, *Nucl. Phys.* **B567**, 189 (2000).
- [55] J. M. Cline, Inflation from extra dimensions, *AIP Conf. Proc.* **488**, 64 (1999).
- [56] J. E. Lidsey, A. R. Liddle, E. W. Kolb, E. J. Copeland, T. Barreiro, and M. Abney, Reconstructing the inflation potential: An overview, *Rev. Mod. Phys.* **69**, 373 (1997).
- [57] R. L. Workman *et al.* (Particle Data Group), Review of particle physics, *Prog. Theor. Exp. Phys.* **2022**, 083C01 (2022).
- [58] L. A. Anchordoqui, Decaying dark matter, the  $H_0$  tension, and the lithium problem, *Phys. Rev. D* **103**, 035025 (2021).
- [59] N. Arkani-Hamed, S. Dimopoulos, and G. R. Dvali, Phenomenology, astrophysics and cosmology of theories with submillimeter dimensions and TeV scale quantum gravity, *Phys. Rev. D* **59**, 086004 (1999).
- [60] A. E. Evrard, Biased cold dark matter theory: Trouble from rich clusters?, *Astrophys. J.* **341**, L71 (1989).
- [61] M. Asgari *et al.* (KiDS Collaboration), KiDS-1000 Cosmology: Cosmic shear constraints and comparison between two point statistics, *Astron. Astrophys.* **645**, A104 (2021).
- [62] T. M. C. Abbott *et al.* (DES Collaboration), Dark energy survey year 3 results: Cosmological constraints from galaxy clustering and weak lensing, *Phys. Rev. D* **105**, 023520 (2022).
- [63] K. Enqvist, S. Nadathur, T. Sekiguchi, and T. Takahashi, Decaying dark matter and the tension in  $\sigma_8$ , *J. Cosmol. Astropart. Phys.* **09** (2015) 067.
- [64] G. Franco Abellán, R. Murgia, and V. Poulin, Linear cosmological constraints on two-body decaying dark matter scenarios and the  $S_8$  tension, *Phys. Rev. D* **104**, 123533 (2021).
- [65] S. Alvi, T. Brinckmann, M. Gerbino, M. Lattanzi, and L. Pagano, Do you smell something decaying? Updated linear constraints on decaying dark matter scenarios, *J. Cosmol. Astropart. Phys.* **11** (2022) 015.
- [66] G. Franco Abellán, R. Murgia, V. Poulin, and J. Laval, Implications of the  $S_8$  tension for decaying dark matter with warm decay products, *Phys. Rev. D* **105**, 063525 (2022).
- [67] T. Simon, G. Franco Abellán, P. Du, V. Poulin, and Y. Tsai, Constraining decaying dark matter with BOSS data and the effective field theory of large-scale structures, *Phys. Rev. D* **106**, 023516 (2022).
- [68] L. Fuß and M. Garny, Decaying dark matter and Lyman- $\alpha$  forest constraints, [arXiv:2210.06117](https://arxiv.org/abs/2210.06117).
- [69] H. Tanimura, M. Douspis, N. Aghanim, and J. Kuruvilla, Can decaying dark matter models be a solution to the  $S_8$  tension from the thermal Sunyaev-Zel'dovich effect?, [arXiv:2301.03939](https://arxiv.org/abs/2301.03939).